Journal of Applied Polymer Science

Silk fibroin nanofibers electrospun on glass fiber as a potential device for solid phase microextraction

Vinícius Müller,[1] Marília Cestari,[2] Soraya M. Palácio,[1] Sílvia D. de Campos,[1] Edvani C. Muniz,[2] Elvio A. de Campos[1]

[1]Center of Engineering and Exact Sciences, UNIOESTE—State University of West Paraná, R. da Faculdade 645, Toledo 85903-000, Paraná, Brazil

[2]Department of Chemistry, UEM—State University of Maringá, Av. Colombo, 5790, Maringá 87020-700, Paraná, Brazil

Correspondence to: E. A. de Campos (E-mail: elvioantonio@uol.com.br)

ABSTRACT: The electrospinning technique was applied to coat fused silica fibers with regenerated silk fibroin (RSF) nanofibers, aiming to build a device applicable for solid phase microextraction analysis. The device was characterized by attenuated total reflectance infrared spectroscopy, thermal analyses (differential scanning calorimetry and thermogravimetric analysis), and scanning electron microscopy, and employed to extract/desorb isopropyl alcohol (IPA) from the headspace of an IPA aqueous solution. The electrospun coating proved to be thermally stable up to 250°C, even after 4 h of exposure to this temperature. A 2^2 factorial experimental design was used to evaluate the flow rate of the polymer solution and the distance between capillary tip and collector on the mean RSF fiber diameter. A low flow rate (0.20 mL h^{-1}) and large capillary tip-to-collector distance (12 cm) yielded fibers with mean diameter of (304 ± 46 nm). The nanofibers were heated to 250°C, simulating the conditions in the injector of a gas chromatograph (GC). In these conditions, the RSF nanofibers were found not to melt even after 4 h of exposure to heat, although slight structural damage was detected. Preliminary assays using the as-constructed device built under optimized electrospinning conditions (0.20 mL h^{-1} and 12 cm) were performed in a GC by contact with the headspace of a 50 ppm IPA solution to determine the extraction and desorption times. The results indicated that the extraction process stabilized after 20 min of contact with the headspace of the IPA solution. The desorption process was complete after 10 min at 140°C. © 2014 Wiley Periodicals, Inc. J. Appl. Polym. Sci. **2015**, *132*, 41717.

KEYWORDS: biopolymers & renewable polymers; electrospinning; fibers; surfaces and interfaces

Received 29 April 2014; accepted 31 October 2014

DOI: 10.1002/app.41717

INTRODUCTION

Solid phase microextraction (SPME) was developed as an alternative to conventional extraction techniques.[1] It precludes the use of organic solvents and sample purification and does away with several extraction stages, further purification and sample concentration, because the SPME technique combines these steps into a single one. In SPME, the adsorbent device consists of a fiber coated with adsorbent material, which serves as an extraction phase. Analytes are extracted and concentrated on the adsorbent surface of the device, a process that is governed by the affinity between the adsorbent and adsorbate. The extraction mechanism is triggered by immersing the adsorbent device directly into the analyte sample or by exposing it to the "headspace" of the sample. Analytes that have an affinity for the adsorbent surface are adsorbed on it until equilibrium is reached. The amount of extracted analyte is a function of the equilibrium constant between the number of adsorbent sites on the coating surface and the analyte concentration.[1] After reaching equilibrium, the adsorbent is then removed from the sample and the analytes are thermally desorbed by further separation and detection by gas chromatography (GC) or by high performance liquid chromatography (HPLC).

The main factors that influence the conditions of equilibrium include the properties of the analyte solution and the intrinsic characteristics of the adsorbent device, such as the thickness and physical and chemical characteristics of the coating film.[2] Thus, different materials provide distinct selectivities and different extraction efficiencies for a given analyte. The existing commercial devices generally consist of fused silica fiber coated with polydimethylsiloxane (PDMS) to extract non-polar compounds, and polyacrylate (PA) to extract polar compounds.[3] Current studies on coatings applied to SPME focus on low cost materials that also present high selectivity and thermal stability and are easy to produce.[4]

Many different methods can be used to produce different coatings applicable for the SPME technique, including electrospinning

of polymer solutions, which offers the advantages of versatility and a wide range of materials that can be used without the need for "glues," leading to reusable materials with large surface areas.

Electrospinning involves the use of a high electric field between a metal capillary (often a needle) containing the polymer solution and a collector (often a large flat metal surface). When the electric field is sufficiently high to induce a charge on the surface of the solubilized polymer chains, droplets of solution deform into a cone, called a Taylor cone, at the tip of the capillary. As the voltage rises, the repulsion between the electrically charged polymer chains increases. Once ejected from the tip of the cone, the polymer chains fall into the collector and are stretched, causing them to become increasingly thinner as the solvent vaporizes, transforming the dry polymer into very fine fibers.[5]

Silk fibroin (SF) is a protein, the main constituent of the cocoon produced by the silkworm (*Bombyx mori*). The chemical structure of SF is thermodynamically stable and soluble in a variety of solvents.[6] The structure is usually composed of β-sheets, with a predominance of hydrophobic domains interspersed with small hydrophilic domains, which make the polymer fibers strong.[7] SF has excellent mechanical properties, thermal stability, biodegradability, and good vapor permeability, which qualify it for use as an extractor for volatile analyte compounds in SPME.

The aim of this work was to prepare and characterize a new device potentially applicable as an adsorbent for the SPME technique, by electrospinning a polymeric coating of fused silica fibers. To this end, a polymer solution of SF protein was electrospun into mats, which were then used for isopropyl alcohol (IPA) extraction from aqueous solutions, combined with detection by GC.

EXPERIMENTAL

Preparation of Regenerated Silk Fibroin

Silkworm (*Bombyx mori*) cocoons (supplied by Cocamar, Maringá, PR, Brazil) were first degummed twice using a 0.5% (w/v) $NaHCO_3$ solution at 100°C for 30 min, and after each degumming step they were washed in distilled water at 70°C. The degummed silk fibroin was then dissolved in a 20/80 (v/v) mixture of $CaCl_2$ 5 mol L^{-1} ethanol/aqueous solution and heated to 80°C for 30 min under stirring. After solubilization, the silk fibroin solution was dialyzed against distilled water for 72 h, using a cellulose acetate membrane and changing the distilled water every 12 h. The dialyzed SF solution was vacuum-filtered, frozen in liquid nitrogen, and freeze-dried to obtain regenerated silk fibroin (RSF) sponges.[8,9]

Preparation of RSF Nanofibers for SPME Devices

A certain amount of RSF was dissolved in formic acid by stirring until it was completely dissolved, forming a 12% (w/v) solution. A given volume of this solution was then transferred to a 10 mL polypropylene syringe with a metal needle (without a tip), which was coupled to a flow controller. A homemade high voltage source (0–30 kV) was connected to the needle tip and to a grounded metallic collector. A mechanical stirrer (13 cm long) containing a 0.380 mm diameter fused silica fiber was placed perpendicularly to the capillary-collector direction 1 cm above the metal collector. The stirring speed was set at 30 rpm. Figure 1 shows a schematic diagram of the electrospinning apparatus. Each electrospun mat was collected after 30 min. The voltage for the electrospinning process was set at 20 kV; three different flow rates (0.20 mL h^{-1}, 0.50 mL h^{-1}, 0.35 mL h^{-1}) and three capillary tip-to-collector distances (7.0 cm, 9.5 cm, and 12.0 cm) were used.[8] After the electrospinning process, fused silica fibers coated with RFS nanofibers were immersed for 24 h in a solution containing methanol to remove any remaining non-adherent nanofibers, after which the final material was dried at room temperature.[10]

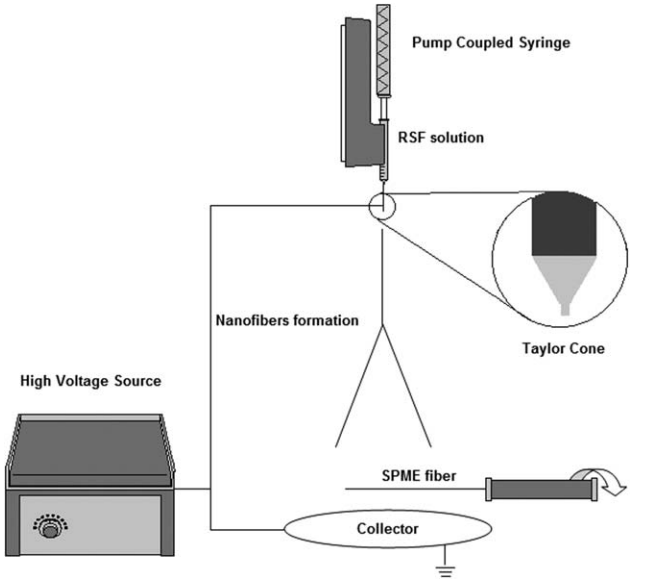

Figure 1. Schematic diagram of the electrospinning apparatus used to produce RSF electrospun nanofibers deposited on fused silica fiber for application in SPME.

2^2 Experimental Design

A 2^2 factorial experimental design was applied to determine the influence of flow rate, capillary tip-to-collector distance, and the interaction between them on the mean diameter of the RSF electrospun fibers (as response). These factors were fixed at two levels: duplicate at axial points and triplicate at the center point (Table I). The lowest and highest flow rates were 0.20 mL h^{-1} and 0.50 mL h^{-1}, respectively. The capillary tip-to-collector distances were 7.0 cm (lower level) and 12.0 cm (upper level). The central point was set at 0.35 mL h^{-1} for flow rate and 9.5 cm for capillary tip-to-collector distance. The experimental data obtained from this 2^2 factorial design were processed using Design Expert® 7.1.3 software. The significance of the factors was confirmed by analysis of variance (ANOVA).

Characterization of RSF Nanofiber SPME Devices

Scanning Electron Microscopy. The fused silica fibers coated with electrospun RSF nanofibers, prepared as described above, were dried, frozen and broken into smaller sections for morphological analysis. After coating the samples with a thin layer of gold, they were analyzed by scanning electron microscopy (SEM) (Shimadzu SS-550). The mean diameter of each type of

Table I. Conditions of Polymeric Solution Flow Rate and Capillary Tip-To-Collector Distance Used in the 2^2 Factorial Experimental Design, and Corresponding Mean Diameters of RSF Electrospun Nanofibers

		Variables		
Experiment	Run	Flow rate (mL h^{-1})	Distance (cm)	Mean diameter (nm)
1	2	0.20	7.0	490
2	9	0.20	7.0	461
3	4	0.50	7.0	520
4	11	0.50	7.0	490
5	10	0.20	12.0	304
6	3	0.20	12.0	310
7	1	0.50	12.0	342
8	7	0.50	12.0	320
9	8	0.35	9.5	399
10	6	0.35	9.5	410
11	5	0.35	9.5	403

each mat was calculated using Size Meter® version 1.1 software (30 fibers were measured, three times each).

Infrared Spectroscopy. RSF electrospun nanofibers, after treatment by immersing in methanol for 24 h, and the not electrospun RSF (pure RSF) were characterized by attenuated total reflectance Fourier transform infrared spectroscopy (ATR-FTIR), using a Bomem MB-100 FTIR spectrometer operating in the range of 4000–400 cm^{-1} with 4 cm^{-1} resolution and 37 acquisitions per minute. Each spectrum was obtained after 64 acquisitions.

Thermal Analyses (Differential Scanning Calorimetry and Thermogravimetric Analysis). Thermal analyses by differential scanning calorimetry (DSC) and thermogravimetric analysis (TGA) were performed using a Netzsch STA 409 PC Luxx® thermogravimetric analyzer (Germany), applying a heating rate of 10°C/min^{-1}, in an atmosphere of nitrogen gas (20 mL min^{-1}) and a temperature range of 22–600°C.

Thermal Treatment of RSF Nanofiber SPME Devices

The devices coated with RSF nanofibers were treated for 1 h at 100°C, 150°C, 200°C, or 250°C in an electric furnace (Fischer Grill, 50°C-320°C, Brazil). They were also heated to 250°C for 3 h and 4 h. After thermal treatment, the morphology of the fibers was evaluated by SEM to check for possible damage.

Chromatographic Assays and Extraction/Desorption Parameters

For the chromatographic assays, an aqueous solution of IPA (density = 0.786 g mL^{-1}) was prepared as follows. 398 µL of IPA were transferred to a 50 mL volumetric flask containing 40 mL of dimethylformamide (DMF) and the flask's volume was completed with DMF. Exactly 1 mL of this solution was transferred to a 25 mL volumetric flask and the volume was completed with DMF. Finally, 1 mL was transferred to a 20 mL vial containing 4 mL of water, totalizing 50 ppm of IPA, and the vial was sealed with a rubber septum and aluminum crimp cap. The incubation condition was 60°C for 40 min. Exactly 5.0 mm of the coated fiber was then exposed to the headspace of the vial. The extraction and desorption times, each varying from 5 to 30 min, were evaluated to obtain the parameters of extraction.

A Varian 3900 gas chromatograph was used, operating with a flame ionization detector (FID); a G43 column (6%-cyanopropylphenyl-94%-dimethylpolysiloxane) 30 m × 0.53 mm × 3 mm coating film; using helium as carrier gas; linear speed: 35 cm s^{-1}; operating in splitless mode. Column temperature was 40°C for 20 min, followed by a heating rate of 10°C min^{-1} to 240°C, where it was held for 20 min. The injector and detector temperatures were maintained at 140°C and 250°C, respectively.

RESULTS AND DISCUSSION

Preliminary Assays and Characterization by SEM

The FTIR spectra of the pure RSF and electrospun RSF presented two intense bands between 1700 and 1500 cm^{-1}, which were attributed to C=O stretching of amides[11] corresponding to type I and type II amides. In the FTIR spectrum of RSF, these bands were observed at 1657 cm^{-1} and 1520 cm^{-1}, respectively, while in the FTIR spectrum of electrospun RSF, these bands were observed at 1621 cm^{-1} and 1508 cm^{-1}, respectively. The shift of the fibers to lower energy regions of the spectrum was attributed to a change in the conformation of the SF fibers from random coils (pure RSF) to β-sheets (electrospun RSF). This can be explained by the rearrangement of the crystal structure of SF chains due to changes in hydrogen bonds caused by contact with chemicals such as methanol and ethanol.[11]

Figure 2 shows SEM micrographs of fused silica fibers coated with RSF. This technique was used to optimize the electrospinning parameters. Considerable differences were found in the morphology of the fiber coatings. Coated fibers prepared by applying a polymer solution flow rate of 0.50 mL h^{-1} and capillary tip-to-collector distance of 9.5 cm [Figure 2(b,c)] showed signs of coalescence (beads) and presented various polymer droplets on the fiber surface, forming a practically condensed surface coating film. This probably occurred because the nanofibers were not totally solvent-free when they were deposited on the fused silica fiber surface, allowing unwanted interaction between RSF nanofibers. This indicates that the polymer solution flow was relatively high for the process or that the capillary tip-to-collector distance was too small.

When the flow rate of the polymer solution was decreased to 0.35 mL h^{-1} and the capillary tip-to-collector distance to 7.0 cm [Figure 2(d,e)], the formation of droplets appeared to be similar to those depicted in Figure 2(b,c), but the coalescence was somewhat intensified. This intensification suggests that capillary tip-to-collector distance is the main factor governing the morphology of RSF nanofibers. Figure 2(f,g) show SEM micrographs of nanofibers obtained at a flow rate of 0.20 mL h^{-1} and capillary tip-to-collector distance of 12.0 cm deposited on fused silica fibers. In Figure 2(g), note that nanofibers appear to be more homogenous than those obtained under the other

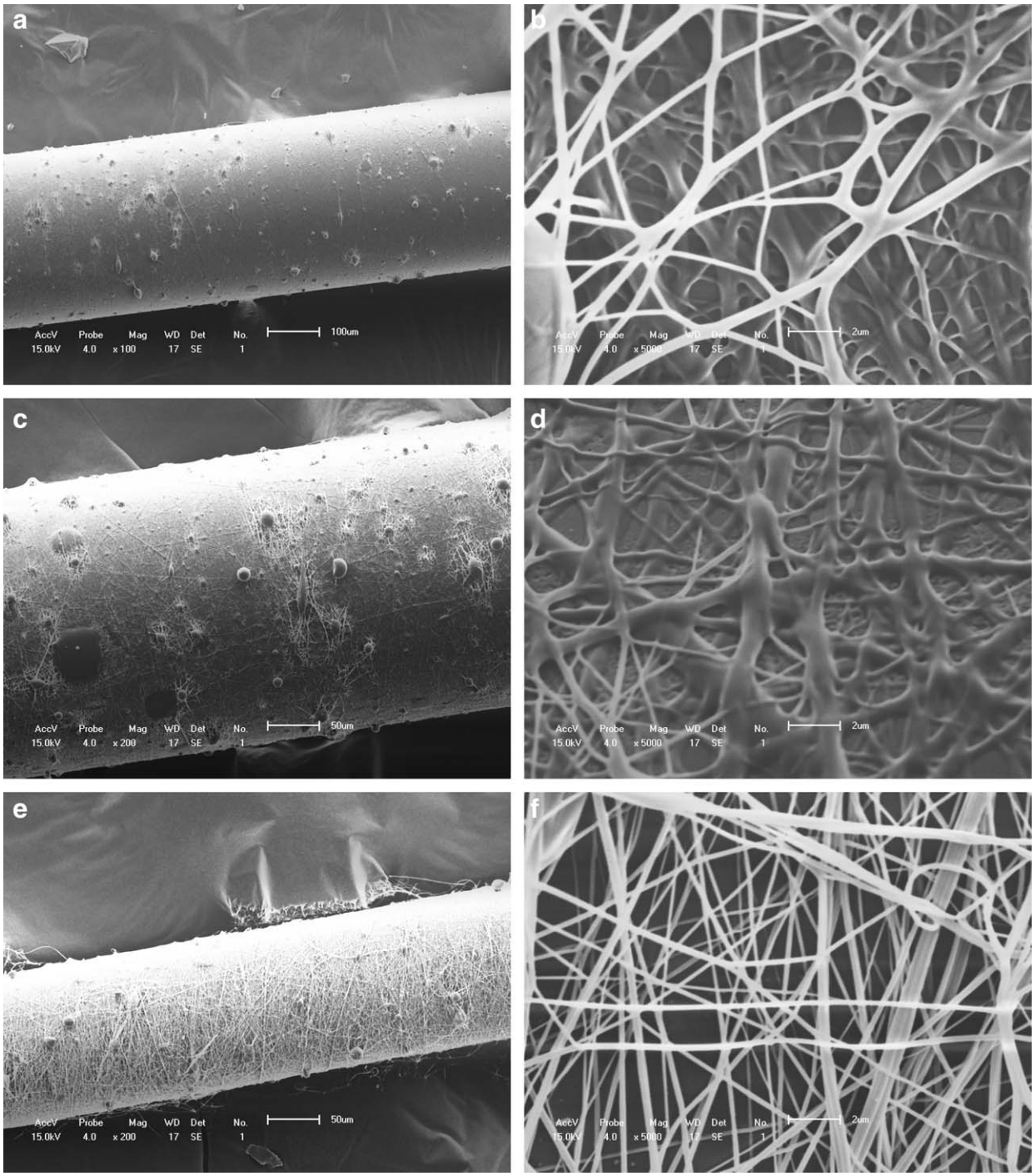

Figure 2. SEM micrographs of: (a) pure fused silica fibers and coated with RSF electrospun nanofibers using flow rate of 0.50 mL h^{-1} and capillary tip-to-collector distance of 9.5 cm under magnification of (b) ×100 and (c) ×5000; flow rate of 0.35 mL h^{-1} and capillary tip-to-collector distance of 7.0 cm under magnification of (d) ×200 and (e) ×5000; flow rate of 0.20 mL h^{-1} and capillary tip-to-collector distance of 12.0 cm under magnification of (f) ×200 and (g) ×5000.

above described conditions [Figure 2(b–e)], with no significant signs of coalescence and only a few agglomeration points [Figure 2(f)]. Using a lower flow rate (0.20 mL h^{-1}) decreases the amount of solvent that must evaporate as the nanofiber travels from the tip of the capillary to the fused silica. Likewise, a concomitant increase in capillary tip-to-collector distance probably allows sufficient time for complete evaporation of the solvent, so the fibers are almost completely dry when they reach the fused silica. This seems to prevent coalescence, so only a few agglomeration points are formed.

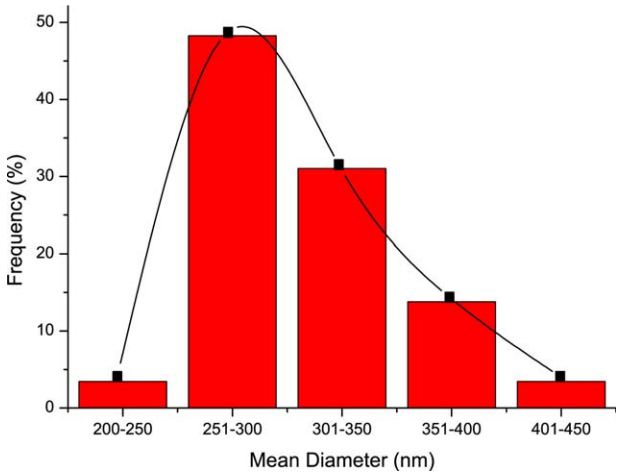

Figure 3. Histogram of the diameters of electrospun RSF nanofibers obtained at a flow rate of 0.20 mL h^{-1} and capillary tip-to-collector distance of 12.0 cm, after 30 min of electrospinning. [Color figure can be viewed in the online issue, which is available at wileyonlinelibrary.com.]

The mean nanofiber diameters were determined from the SEM micrographs of the fused silica coated with RSF electrospun nanofibers, using Size Meter® version 1.1 software. The RSF electrospun fibers obtained at a flow rate of 0.20 mL h^{-1} and capillary tip-to-collector distance of 12.0 cm showed a mean diameter of 304 ± 46 nm, that is, they are nanofibers (smaller than 1000 nm).[12] Figure 3 shows a histogram of the diameters of nanofibers deposited on a fused silica fiber under the optimized electrospinning conditions (flow rate 0.20 mL h^{-1} and capillary tip-to-collector distance 12.0 cm). The distribution in Figure 3 shows a unimodal profile with a higher occurrence of nanofiber diameters in the range of 250–300 nm.

Although the physical dimensions of fused silica fiber coated with RSF do not allow the exact determination of specific surface area, this material certainly has a large surface area in view of the small diameter of the coated nanofibers. This suggests that a large amount of analyte can be extracted by this adsorbent material, which is desirable for SPME devices.

2^2 Experimental Design

Table I lists the values of the mean diameters of RSF electrospun nanofibers measured in each run of the 2^2 factorial experimental design and describes the conditions used in each run. Note that the process is highly reproducible, as indicated by the low variations of the replicated runs. The largest mean diameter of RSF electrospun fibers was obtained (505 nm) using the smaller capillary tip-to-collector distance (7.0 cm) and higher flow rate of the polymer solution (0.50 mL h^{-1}). On the other hand, as mentioned, the smallest mean diameter (307 nm) was obtained at the greater capillary tip-to-collector distance (12.0 cm) and lower flow rate (0.20 mL h^{-1}).

The significance of the factors was confirmed by the variance analysis (ANOVA) presented in Table II. Both the factors (flow rate and capillary tip-to-collector distance) were statistically significant ($P < 0.05$). The capillary tip-to-collector distance seems to be the most important factor that affects the mean diameter. The interaction between variables and curvature of the model were not significant ($P > 0.05$). A linear model eq. (1) was built by regression analysis, and describes the relationship between the response (mean fiber diameter) and significant factors (flow rate and capillary tip-to-collector distance). The results presented in Table II indicate that this model was significant ($F_{2,6} = 174.14$ and $P < 0.05$), and the lack of fit was not significant ($P > 0.05$). These data indicate that the model is robust in explaining the experimental observations; $R^2_{pred} = 0.949$ are in accordance with $R^2_{adj} = 0.974$, confirming this result.

The linear model was built by regression analysis, and describes the relationship between the significant independent variables and the response, as indicated by eq. (1).

$$\text{Diameter (nm)} = 699 + 89 \times \text{Flow rate (mL h}^{-1}\text{)} - 34 \times \text{Distance (cm)} \quad (1)$$

The positive coefficient for flow rate and negative for capillary tip-to-collector distance are consistent with the discussion of the SEM micrographs. Thus, a low flow rate and large capillary tip-to-collector distance are required to produce fibers with small diameters.

The data normality was verified by examining the distribution of residuals (difference between the experimental values and those predicted by regression). The analysis of the residual plot (not shown) indicated that the residuals were randomly distributed around zero, indicating normal distribution, and hence, equality of variances in the results. The random distribution of the residuals indicated that the normality assumption was satisfied. There was no presence of outliers, since all the values fell within the acceptable range (from −3 to 3). The $R^2 = 0.980$

Table II. Variance Analysis (ANOVA) of the Response Surface of the Linear Model, Based on Mean RSF Fiber Diameter

Source	Sum of squares	Degrees of freedom	Mean square	*F*-value	*P*-value
Model	60,084.25	2	30,042.12	174.14	<0.0001
Flow rate(mL h^{-1})	1431.12	1	1431.12	8.30	0.0236
Distance (cm)	58,653.13	1	58,653.13	339.98	<0.0001
Curvature	0.85	1	0.85	4.940E-003	0.9459
Residual	1207.63	7	172.52		
Lack of fit	15.13	1	15.13	0.076	0.7919
Pure error	1192.50	6	198.75		
Total	61,292.73	10			

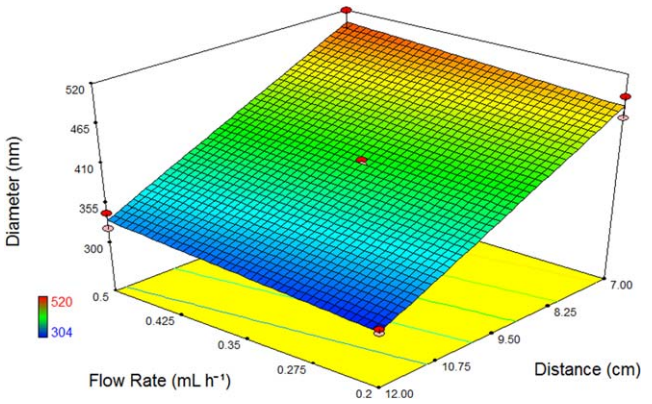

Figure 4. Response surface of experimental results of the factorial design 2^2. The response is the mean diameter of RSF electrospun fibers measured at three polymer solution flow rates and capillary tip-to-collector distances in the electrospinning process. [Color figure can be viewed in the online issue, which is available at wileyonlinelibrary.com.]

confirmed the validation of the model. Figure 4 shows the response surface obtained after applying the model.

Thermal Analysis

In the thermal desorption process on SPME, like in the GC, the devices were subjected to high temperatures in the injector. Since we were dealing with biopolymer-based nanofibers, there was concern for possible structural damage that might result from the application of high temperature.

To verify the potential applicability of the as-obtained device in SPME, electrospun RSF mats deposited on fused silica were subjected to thermal analyses. Figure 5 shows DSC and TGA results. This figure shows TGA curves (red and black lines) of pure RSF and RSF electrospun nanofibers deposited on the surface of fused silica. As can be seen, the thermal stability of the RSF is practically the same in both cases (pure RSF and RSF electrospun nanofibers), and is somewhat more thermally resistant when deposited on the surface of the glass fiber. Two

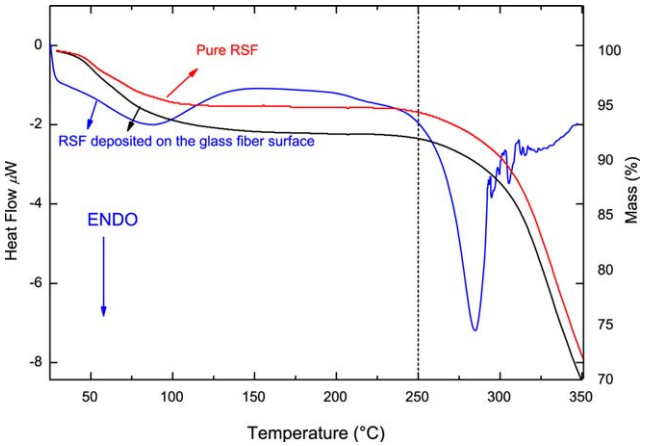

Figure 5. TGA curves of pure RSF, and TGA and DSC curves of RSF electrospun nanofibers deposited on the fused silica surface (0.20 mL h^{-1} and 12 cm). [Color figure can be viewed in the online issue, which is available at wileyonlinelibrary.com.]

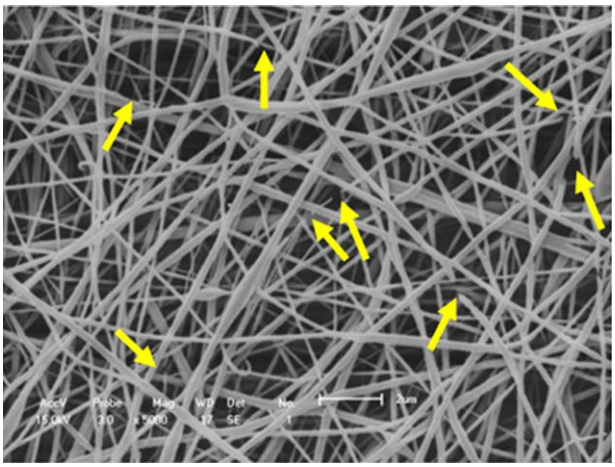

Figure 6. SEM micrograph of RSF electrospun nanofibers deposited on fused silica fiber surface and further exposed to heat treatment at 250°C for 4 h. [Color figure can be viewed in the online issue, which is available at wileyonlinelibrary.com.]

different regions of mass loss are visible: the first, which goes up to about 100°C, is due to water loss and methanol adsorbed on polymer chains. The second region, which ranges from 250 to 350°C, is associated with the degradation of residues of amino acid side groups and the cleavage of peptide bonds[13,14] of fibroin. These phenomena are evidenced by the endothermic peaks shown in the DSC curve (blue line). In the DSC curve from RSF deposited on the glass fiber there is no crystallization peak, as observed in films of silk fibroin cast from fibroin–water solutions.[15] Except for the endothermic peaks below 300°C, there is little similarity between the DSC curve of RSF deposited on glass fiber and the DSC curve of films of silk fibroin cast from fibroin–water solutions: the glass transition temperature of the RSF nanofibers is close to 205°C, which is higher than that observed for films of silk fibroin (170–190°C).[15] The low intensity endothermic peaks above 300°C are not observed in DSC curves of silk fibroin films and

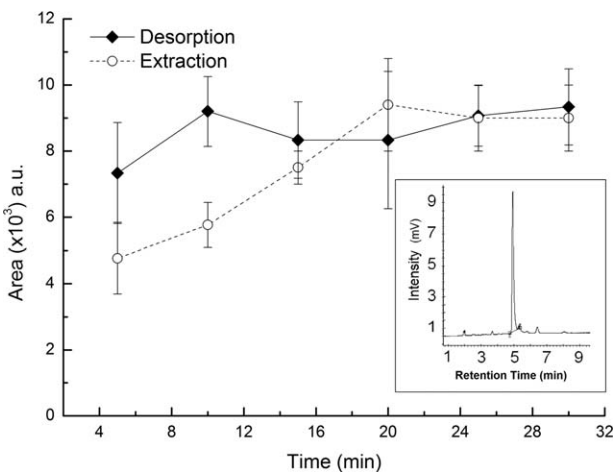

Figure 7. Area in the GC chromatogram at different extraction/desorption times. The extraction was performed with the as-prepared SPME device in contact with the headspace of 50 ppm aqueous solution of IPA.

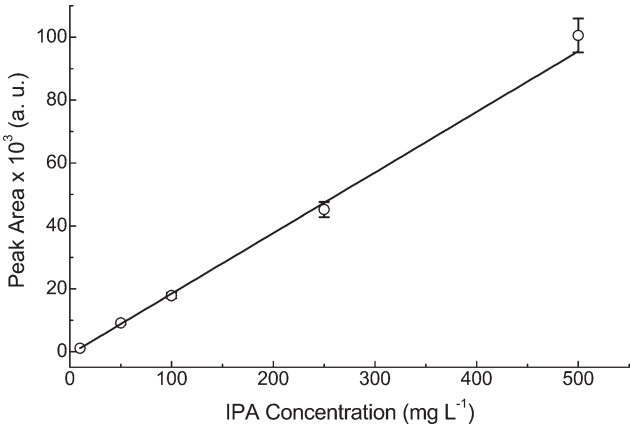

Figure 8. Area in the GC chromatogram at different concentration of IPA performed with the extraction times of 20 min and desorption times of 10 min.

are probably related to the thermal decomposition of intermediary organic compounds formed by the decomposition of RSF nanofibers, since no modification of the silica glass fiber occurs at this temperature.

It is apparent, from the thermal analyses, that the temperature range extending up to around 250°C can be used in the SPME desorption process without melting or loss of material through degradation.

In order to simulate SPME temperature conditions of a gas chromatograph injector, the devices were heat-treated, respecting the temperature limitations of possible RSF thermal decomposition. The fused silica fibers coated with RSF electrospun nanofibers in the optimized conditions (0.20 mL h^{-1} and 12 cm), were heat-treated at 100°C, 150°C, 200°C, and 250°C for 1 h, and at 250°C for 3 h and 4 h. No significant changes were observed after any of these thermal treatments. Figure 6 shows a SEM micrograph of the fused silica fiber coated with RSF electrospun nanofibers after undergoing the most severe heat treatment: 4 h at 250°C.

The arrows in Figure 6 indicate breaks observed in some RFS nanofibers, which is the only damage observed after thermal treatment. The RFS nanofibers in the other heat-treated samples showed the same type of break, with similar frequency, which occurred even when exposed to 100°C for 1 h. This finding confirms that, under these conditions, this material is potentially applicable as a SPME device, without major changes in the external morphology of RSF electrospun nanofibers.

Chromatographic Assays

The potential use of the as-obtained device in SPME combined with GC was tested using 50 ppm of IPA aqueous solution. Figure 7 depicts the results of chromatographic assays, showing the peak area of the analyte (IPA) (in the GC chromatogram at an elution time of about 5 min, see, e.g., the inset in Figure 7) as a function of extraction/desorption time. The results indicate that, to reach equilibrium, the device required a minimum contact time of 20 min with the headspace of the IPA solution. Thus, the extraction time was set for 20 min and the desorption time varied from 5 to 30 min. Note that there was no appreciable variation in the analyte peak area after the device was left in the injector for 10 min or longer at 140°C.

This extraction time is slightly shorter than that required to extract the same analyte using commercial SPME devices (about 30 min).[16] However, the desorption occurred in 10 min, while the desorption of IPA, as well as that of the other analytes, using commercial devices occurs in only 1 min. An important point to keep in mind is the difference in injector temperature in these two studies: the temperature used here was 140°C, and the injector temperature using the commercial devices was 250–300°C.

Figure 8 shows the result of the linearity assay performed in triplicate at optimized extraction and desorption times, with IPA concentrations of 10–500 mg L^{-1}. The peak areas in the chromatograms show a good linear correlation with the concentration, with $R^2 = 0.9973$ at an extraction time of 20 min and desorption time of 10 min.

CONCLUSIONS

Fused silica fibers were coated with electrospun RSF nanofibers and the experimental design indicated that a low flow rate of the polymer solution and large capillary tip-to-collector distance are required to produce nanofibers with small diameters. The newly built device, operating at the optimized polymer solution flow rate and capillary tip-to-collector distance, proved to be thermally stable up to 250°C and is potentially applicable in analytical studies involving solid-phase microextraction with IPA.

ACKNOWLEDGMENTS

The authors are grateful to the pharmaceutical company Prati-Donaduzzi (Brazil) for making its gas chromatograph available for our use.

REFERENCES

1. Pawliszyn, J. In Handbook of Solid Phase Microextraction, 1st ed.; Pawliszyn, J., Ed.; Elsevier: USA, **2012**; pp 2–12.
2. Zewe, J. W.; Steach, J. K.; Olesik, S. V. *Anal. Chem.* **2010**, *82*, 5341.
3. Shirey, R. E. In Handbook of Solid Phase Microextraction, 1st ed.; Pawliszyn, J., Ed.; Elsevier: USA, **2012**; pp 99–133.
4. Dietz, C.; Sanz, J.; Camara, C. *J. Chromatogr. A* **2006**, *1103*, 183.
5. Ramakrishna, S.; Fujihara, K.; Teo, W. E.; Lim, T. C.; Ma, Z. An Introduction to Electrospinning and Nanofibers; World Scientific Publishing Co. Pte. Ltd.: Singapore, **2005**.
6. Ha, S. W.; Gracz, H. S.; Tonelli, A. E.; Hudson, S. M. *Biomacromolecules* **2005**, *6*, 2563.
7. Vepari, C.; Kaplan, D. L. *Prog. Polym. Sci.* **2007**, *32*, 991.
8. Wang, S.; Zhang, Y.; Wang, H.; Dong, Z. *Int. J. Biol. Macromol.* **2011**, *48*, 345.

9. Miyaguchi, Y.; Hu, *J. Food Sci. Technol. Res.* **2005**, *11*, 37.
10. Cestari, M.; Muller, V.; Rodrigues, J. H.; Nakamura, C. V.; Rubira, A. F.; Muniz, E. C. *Biomacromolecules* **2014**, *15*, 1762.
11. Yin, G. B.; Zhang, Y. Z.; Bao, W. W.; Wu, J. L.; Shi, D. B.; Dong, Z. H.; Fu, W. G. *J. Appl. Polym. Sci.* **2009**, *111*, 1471.
12. Zhou, F.-L.; Gong, R.-H. *Polym. Int.* **2008**, *57*, 837.
13. Nogueira, G. M.; Rodas, A. C. D.; Leite, C. A. P.; Giles, C.; Higa, O. Z.; Polakiewicz, B.; Beppu, M. M. *Bioresource Technol.* **2010**, *101*, 8446.
14. Um, I. C.; Kweon, H. Y.; Park, Y. H.; Hudson, S. *Int. J. Biol. Macromol.* **2001**, *29*, 91.
15. Motta, A.; Fambri, L.; Migliaresi, C. *Macromol. Chem. Phys.* **2002**, *203*, 1658.
16. Camarasu, C. C. *J. Pharm. Biomed. Anal.* **2000**, *23*, 197.